The Canadian Mineralogist
Vol. 36, pp. 1245-1252 (1998)

SYNTHETIC FLUORO-AMPHIBOLES: SITE PREFERENCES OF Al, Ga, Sc AND INDUCTIVE EFFECTS ON MEAN BOND-LENGTHS OF OCTAHEDRA

ROBERTA OBERTI[1], FRANK C. HAWTHORNE[2] AND FERNANDO CAMARA[3]

CNR – Centro di Studio per la Cristallochimica e la Cristallografia (CSCC), via Ferrata 1, I-27100 Pavia, Italy

MATI RAUDSEPP

Department of Earth and Ocean Sciences, University of British Columbia, Vancouver, British Columbia V6T 1Z4

ABSTRACT

The crystal structure and site populations of four synthetic amphiboles of nominal M^{3+}-substituted fluoro-magnesiokatophorite ($NaCaNaMg_4M^{3+}Si_7AlO_{22}F_2$, M^{3+} = Al, Ga, Sc) and Ga-substituted fluoropargasite ($NaCa_2Mg_4GaSi_6Al_2O_{22}F_2$) compositions have been refined to R indices of 1–3% using intensity data collected with Mo$K\alpha$ X-radiation. The crystals used in the collection of the X-ray data were subsequently analyzed with an electron microprobe. Both techniques confirm significant deviations from the expected stoichiometry. Octahedrally coordinated trivalent cations are totally ordered at the $M(2)$ site. In the Ga-bearing crystals, Ga and Al occur in both octahedral and tetrahedral coordination (*i.e.*, there is Ga–Al disorder between the M and T sites); in Ga-bearing fluoro-magnesiokatophorite, tetrahedrally coordinated Ga and Al are completely ordered at the $T(1)$ site, whereas in Ga-bearing fluoropargasite, Ga is partly disordered over $T(1)$ and $T(2)$, and Al is ordered at $T(1)$. Therefore, only the fraction of Ga occurring in octahedral coordination in amphiboles should be used to calculate partition coefficients to be compared to those of the other $^{[6]}M^{3+}$ lithophile elements of interest in geochemical studies. In the M^{3+}-substituted fluoro-magnesiokatophorite crystals, ^{A}Na is ordered at the $A(m)$ site, whereas in Ga-substituted fluoropargasite, ^{A}Na and ^{A}Ca are disordered between $A(m)$ and $A(2)$, in accord with the model of Hawthorne *et al.* (1996). Examination of the available data on synthetic fluoro-amphiboles shows that there are significant and systematic variations in <Mg–O,F> both at $M(1)$ and $M(3)$ as a function of bulk composition. These variations can be rationalized as structural strain in response to misfit between the strip of octahedra and the chain of tetrahedra.

Keywords: amphibole, fluoro-magnesiokatophorite, fluoropargasite, synthesis, crystal structure, cation order.

SOMMAIRE

Nous avons affiné la structure cristalline et la population des sites de quatre échantillons synthétiques d'amphibole ayant pour composition nominale la fluoro-magnésiokatophorite, $NaCaNaMg_4M^{3+}Si_7AlO_{22}F_2$ avec incorporation d'ions trivalents (M^{3+} = Al, Ga, Sc), et la fluoropargasite, $NaCa_2Mg_4GaSi_6Al_2O_{22}F_2$, avec incorporation de Ga. Ces affinements de données d'intensité prélevées avec rayonnement Mo$K\alpha$ ont atteint un résidu R dans l'intervalle 1–3%. Les mêmes cristaux ont ensuite été analysés avec une microsonde électronique. Les deux techniques confirment la présence d'écarts importants à la stoechiométrie attendue. Les cations trivalents à coordinence octaédrique sont inmanquablement situés sur le site $M(2)$. Dans le cas des cristaux contenant du gallium, les ions Ga et Al sont répartis entre sites à coordinence tétraédrique (sites T) et octaédrique (sites M). Dans le cas de la fluoro-magnésiokatophorite dopée avec le Ga, les cations Ga et Al à coordinence tétraédrique sont complètement ordonnés sur le site $T(1)$, tandis que dans la fluoropargasite dopée au gallium, le Ga est partiellement désordonné sur $T(1)$ et $T(2)$, et l'Al se trouve ordonné sur $T(1)$. On ne devrait se servir, pour calculer des coefficients de partage et pour fins de comparaison avec d'autres minéraux contenant $^{[6]}M^{3+}$, que de la fraction du Ga qui se trouve en coordinence octaédrique dans les amphiboles. Dans les cristaux de fluoro-magnésiokatophorite dopés avec des ions $^{[6]}M^{3+}$, le ^{A}Na est ordonné sur le site $A(m)$, tandis que dans la fluoropargasite dopée au gallium, le ^{A}Na et le ^{A}Ca sont désordonnés sur les sites $A(m)$ et $A(2)$, selon les prédictions de Hawthorne *et al.* (1996). Une évaluation des données disponibles à propos des fluoro-amphiboles synthétiques montre qu'il y a des variations importantes et systématiques en <Mg–O,F> aux sites $M(1)$ et $M(3)$ en fonction de la composition globale. Ces variations seraient dues aux contraintes structurales causées par le décalage dimensionnel entre le ruban d'octaèdres et la chaîne de tétraèdres.

(Traduit par la Rédaction)

Mots-clés: amphibole, fluoro-magnésiokatophorite, fluoropargasite, synthèse, structure cristalline, degré d'ordre des cations.

---

[1] *E-mail address*: oberti@crystal.unipv.it

[2] Currently at: Department of Geological Sciences, University of Manitoba, Winnipeg, Manitoba R3T 2N2.

[3] Present address: Department of Geology, Arizona State University, Tempe, Arizona 85827-1404, U.S.A.

INTRODUCTION

Lithophile transition-elements such as V, Cr, Ga, Sc and In usually occur in very minor amounts in amphiboles; however, they are widely used in geochemical studies of petrogenetic processes. Understanding their site preference and partitioning as a function of P, T, *X* conditions of crystallization is important, not only to extend our knowledge on amphibole crystal-chemistry to minor constituents, but also to provide reliable crystal-chemical models for the interpretation of solid/solid and solid/liquid partition coefficients ($^{s/l}D$ and $^{s/s}D$) for minor and trace elements. This goal is more easily achieved by working on synthetic amphiboles of simple composition containing large amounts of the normally minor or trace cations.

We recently reported single-crystal structure refinements of synthetic amphiboles of nominal M^{3+}-substituted fluoro-eckermannite (sodic) composition ($NaNa_2Mg_4M^{3+}Si_8O_{22}F_2$), with M^{3+} representing Al, V, Cr, Ga, Sc; Al, V, Cr, Ga and Sc strongly order at the *C*-group *M*(2) site. However, significant deviations from the nominal composition were noted, some Mg occurring in the *M*4 cavity (^{B}Mg, cummingtonite component) in all the samples; for $^{C}M^{3+}$ = Al, V and Ga, ^{B}Mg was invariably found to be around 1 atom per formula unit (*apfu*), and only very low $^{C}M^{3+}$ contents were obtained. The resulting charge arrangement was that of richterite, but important geometrical differences were found owing to the presence of a smaller [6 + 2]-coordinated cation at the *M*(4') site (Oberti *et al.* 1999).

The present paper deals with nominal fluoro-magnesiokatophorite ($NaNaCaMg_4M^{3+}Si_7AlO_{22}F_2$) and fluoropargasite ($NaCa_2Mg_4M^{3+}Si_6Al_2O_{22}F_2$) compositions, *i.e.*, with sodic–calcic and calcic amphiboles that allow trivalent cations at the *T* sites. It thus provides characterization of $^{C}M^{3+}$ ordering in other amphibole groups, and also allows investigation of possible partitioning of trivalent cations over octahedrally and tetrahedrally coordinated sites. Raudsepp *et al.* (1987) reported $^{C}M^{3+}$ ordering in synthetic substituted (M^{3+} = Al, Sc, Cr, Ga) pargasite and fluoropargasite studied by Rietveld refinement and ^{29}Si MAS NMR (for Sc-substituted fluoropargasite); their results indicated very low contents of the $^{C}M^{3+}$ transition metal, and complete ordering of M^{3+} at *M*(2) in fluoropargasite. However, refinement of the structure using Rietveld analysis did not allow the detection of ordering of Al ($Z = 13$) with respect to Mg ($Z = 12$) and Si ($Z = 14$), as the refined <*M*,*T*–O> distances are very imprecise [this issue is discussed in more detail in Oberti *et al.* (1999)]. The single-crystal refinements (SREF) of the present work were obtained from the run products of Raudsepp *et al.* (1987); unfortunately, not all the available samples gave crystals of size suitable for single-crystal data collection with conventional (sealed-tube or rotating-anode) X-ray generators. Here, the new data are compared to other available data to obtain more general conclusions on the crystal chemistry of fluoro-amphiboles.

TABLE 1. SAMPLE CODES AND NOMINAL COMPOSITIONS FOR THE CRYSTALS OF THIS WORK

	Sample Code	SEQ*	Nominal composition	Yields (Amp)
A(1)	FKA A 16	759	$NaCaNaMg_4AlSi_7AlO_{22}F_2$	60–80%
A(2)	FScKA A2 n.1	776	$NaCaNaMg_4ScSi_7AlO_{22}F_2$	50–70%
A(3)	FGaKA A2 n.11	771	$NaCaNaMg_4GaSi_7AlO_{22}F_2$	~50%
A(4)	FGaPA A2	770	$NaCa_2Mg_4GaSi_6Al_2O_{22}F_2$	85%

* SEQ = sequence number in Pavia amphibole data base

EXPERIMENTAL

Synthesis

Dry mixtures of nominal fluoro-amphibole stoichiometry were prepared from commercial reagent-grade oxides and other compounds (NaF, CaF_2, MgO, γ–Al_2O_3, Sc_2O_3, Ga_2O_3, SiO_2 glass) according to the nominal compositions specified in Table 1. After weighing out components, mixtures were blended by hand for 5 minutes and ground in a mechanized alumina mortar under alcohol for 1 hour. Mixtures were dried overnight at 400°C. Fluoro-amphibole charges consisted of 20 to 40 mg of mix and were sealed by welding into flattened 4 × 23 mm Pt tubes. The experiments were done at 1 atm, starting at 1200°C and cooled to 770°C at a cooling rate of 1.2°C/h for 15 days. As these were intended as reconnaissance experiments, no attempt was made to control oxygen fugacity or anneal the charges for any time at 770°C. Further experimental details are given by Raudsepp *et al.* (1991). Codes and nominal compositions for the samples for which SREF data could be obtained are reported in Table 1.

X-ray data collection and structure refinement

The procedures of Oberti *et al.* (1999) were used for data collection and structure refinement. Unit-cell dimensions and other information on the structure refinement are reported in Table 2, atomic coordinates and equivalent isotropic-displacement factors in Table 3, selected interatomic distances and angles in Table 4, and refined site-scattering values in Table 5. A comparison between the refined site-scattering values and those calculated from the unit formula is also reported in Table 5. Observed and calculated structure-factors may be obtained from the Depository of Unpublished Data, CISTI, National Research Council of Canada, Ottawa, Ontario K1A 0S2.

Electron-microprobe data and recalculation of the formulae

The crystals used for SREF analysis were mounted in epoxy and analyzed with a Cameca SX–50 electron microprobe according to the procedure of Raudsepp *et al.* (1991). Ten points were analyzed, and the average composition is given in Table 6. Formula recalculation was first tried assuming 24 (O, F) *apfu*, but the calculated F was always too high, suggesting a problem in the determination of F. Formulae recalculated by fixing F at 2 *apfu* fit much better with the results of structure refinement. For crystals A(3) and A(4), the Al content was not sufficient to fill the tetrahedral sites; Al and Ga were partitioned between the tetrahedral and octahedral sites according to the SREF (site scattering and mean bond-length) results.

TABLE 2. UNIT-CELL DIMENSIONS AND MISCELLANEOUS DATA CONCERNING STRUCTURE REFINEMENTS

	A(1)	A(2)	A(3)	A(4)
a (Å)	9.845(3)	9.853(3)	9.866(3)	9.850(4)
b (Å)	18.010(5)	18.061(8)	17.998(4)	17.934(8)
c (Å)	5.275(1)	5.295(2)	5.285(2)	5.301(2)
β (°)	104.74(2)	104.49(3)	104.93(2)	105.32(4)
V (Å^3)	904.5	912.3	906.8	903.1
sin θ/λ (Å^{-1})	0.70	0.70	0.70	0.70
No. *F* (all)	1369	1386	1373	1371
No. *F* (obs)	831	984	961	1009
R (sym) %	2.6	1.6	1.5	1.4
R (obs) %	1.9	1.4	2.9	1.5
R (all) %	5.6	2.7	4.5	2.7

Space group: *C*2/*m*.

TABLE 3. ATOMIC COORDINATES AND EQUIVALENT ISOTROPIC-DISPLACEMENT FACTORS (Å^2)

		A(1)	A(2)	A(3)	A(4)
O(1)	*x*	0.1116	0.1118	0.1107	0.1072
	y	0.0846	0.0848	0.0850	0.0868
	z	0.2193	0.2184	0.2195	0.2177
	B_{eq}	0.45	0.51	0.56	0.66
O(2)	*x*	0.1188	0.1193	0.1194	0.1185
	y	0.1698	0.1683	0.1704	0.1718
	z	0.7266	0.7268	0.7287	0.7345
	B_{eq}	0.54	0.58	0.56	0.62
O(3)	*x*	0.1034	0.1023	0.1039	0.1035
	z	0.7128	0.7124	0.7133	0.7127
	B_{eq}	0.74	0.72	0.68	0.77
O(4)	*x*	0.3640	0.3621	0.3640	0.3668
	y	0.2488	0.2486	0.2496	0.2514
	z	0.7901	0.7927	0.7883	0.7879
	B_{eq}	0.73	0.80	0.84	0.86
O(5)	*x*	0.3489	0.3490	0.3490	0.3522
	y	0.1351	0.1328	0.1370	0.1409
	z	0.1009	0.0939	0.1052	0.1160
	B_{eq}	0.85	1.00	1.12	1.02
O(6)	*x*	0.3456	0.3455	0.3457	0.3463
	y	0.1173	0.1172	0.1166	0.1161
	z	0.5962	0.5925	0.6016	0.6131
	B_{eq}	0.78	0.85	0.97	1.04
O(7)	*x*	0.3436	0.3437	0.3440	0.3451
	z	0.2871	0.2859	0.2814	0.2766
	B_{eq}	0.79	0.92	1.05	1.05
T(1)	*x*	0.2816	0.2826	0.2820	0.2824
	y	0.0841	0.0843	0.0844	0.0851
	z	0.2990	0.2969	0.3019	0.3054
	B_{eq}	0.36	0.40	0.47	0.42
T(2)	*x*	0.2890	0.2891	0.2894	0.2911
	y	0.1714	0.1704	0.1720	0.1733
	z	0.8057	0.8026	0.8087	0.8153
	B_{eq}	0.42	0.46	0.48	0.51
M(1)	*y*	0.0886	0.0883	0.0889	0.0892
	B_{eq}	0.45	0.49	0.43	0.44
M(2)	*y*	0.1765	0.1787	0.1765	0.1757
	B_{eq}	0.48	0.59	0.57	0.44
M(3)	B_{eq}	0.50	0.49	0.46	0.41
M(4)	*y*	0.2775	0.2781	0.2781	0.2794
	B_{eq}	0.78	1.14	0.78	0.76
A	B_{eq}	1.35	2.01	1.94	2.19
A(*m*)	*x*	0.0421	0.0437	0.0373	0.0398
	z	0.0979	0.1012	0.0936	0.0914
	B_{eq}	2.93	2.59	1.96	2.35
A(2)	*y*	0.4727	0.4730	0.4739	0.4717
	B_{eq}	3.07	3.10	2.10	2.07

Note: standard deviations are ≤1 in the final digit; O(3) = *x*, 0, *z*; O(7) = *x*, 0, *z*; *M*(1) = 0, *y*, 1/2; *M*(2) = 0, *y*, 0; *M*(3) = 0, 0, 0; *M*(4) = 0, *y*, 1/2; *A* = 0, 1/2. 0; *A*(*m*) = *x*, 1/2, *z*; *A*(2) = 0, *y*, 0.

Comparison with nominal compositions

Fluoro-magnesiokatophorite samples A(1) and A(3) are significantly off-composition (Table 7). The very low $^{C}M^{3+}$ contents are compensated by high ^{B}Ca contents in both crystals. Gallium shows a preference for tetrahedral coordination in A(3) and A(4). The deviations from the expected stoichiometry and charge distribution are largest in crystal A(1), which actually falls in the compositional field of fluoro-edenite.

SITE POPULATIONS AND ORDERING

B-group sites

The deviations from the expected *B*-site stoichiometry in crystals A(1)–A(3) are due mainly to the ^{B}(Ca,Mg) + ^{C}Mg → ^{B}Na + $^{C}M^{3+}$ substitution. However, no residual maxima corresponding to the [6 + 2]-coordinated *M*(4') position were found in the difference-Fourier map at convergence, and low values were observed for B_{eq} at *M*(4) and at the coordinating O(4), O(5) and O(6) anions; both these facts are in accord with no (or very low) ^{B}Mg occupancies. Thus the charge arrangement is analogous to that of the fluoro-amphiboles with ^{B}Mg around 1 *apfu* described in Oberti *et al.* (1999), but the availability of Ca in the starting material leads to Ca instead of Mg as the principal divalent *B*-group cation.

TABLE 4. SELECTED INTERATOMIC DISTANCES (Å) AND ANGLES (°)

		A(1)	A(2)	A(3)	A(4)
T(1)–O(1)		1.619	1.629	1.634	1.664
T(1)–O(5)		1.651	1.644	1.663	1.688
T(1)–O(6)		1.645	1.644	1.652	1.680
T(1)–O(7)		1.641	1.644	1.651	1.669
<*T*(1)–O>		1.639	1.640	1.650	1.675
T(2)–O(2)		1.621	1.621	1.621	1.640
T(2)–O(4)		1.590	1.591	1.595	1.613
T(2)–O(5)		1.653	1.653	1.650	1.653
T(2)–O(6)		1.672	1.667	1.677	1.674
<*T*(2)–O>		1.634	1.633	1.636	1.645
M(1)–O(1)	x2	2.057	2.064	2.056	2.047
M(1)–O(2)	x2	2.055	2.051	2.066	2.082
M(1)–O(3)	x2	2.064	2.063	2.070	2.065
<*M*(1)–O>		2.059	2.059	2.064	2.065
M(2)–O(1)	x2	2.154	2.188	2.144	2.086
M(2)–O(2)	x2	2.079	2.088	2.080	2.053
M(2)–O(4)	x2	2.018	2.008	2.011	1.978
<*M*(2)–O>		2.083	2.095	2.079	2.039
M(3)–O(1)	x4	2.054	2.064	2.056	2.055
M(3)–O(3)	x2	2.029	2.026	2.037	2.044
<*M*(3)–O>		2.046	2.051	2.050	2.052
M(4)–O(2)	x2	2.419	2.460	2.424	2.421
M(4)–O(4)	x2	2.324	2.353	2.329	2.326
M(4)–O(5)	x2	2.744	2.797	2.704	2.596
M(4)–O(6)	x2	2.560	2.550	2.573	2.578
A–O(5)	x4	2.970	2.930	3.005	3.059
A–O(6)	x4	3.108	3.132	3.083	3.032
A–O(7)	x2	2.419	2.414	2.400	2.379
A(*m*)–O(5)	x2	3.091	3.066	3.097	3.154
A(*m*)–O(5)	x2	2.957	2.913	3.008	3.057
A(*m*)–O(6)	x2	2.716	2.723	2.716	2.668
A(*m*)–O(7)		2.411	2.409	2.366	2.374
A(*m*)–O(7)		3.152	3.156	3.208	3.241
A(*m*)–O(7)		2.559	2.563	2.549	2.502
A(2)–O(5)	x2	2.582	2.546	2.634	2.655
A(2)–O(6)	x2	2.797	2.825	2.785	2.708
A(2)–O(7)	x2	2.468	2.463	2.446	2.433
O(5)–O(6)–O(5)		166.1	164.7	164.2	160.8
O(3)–*M*(1)–O(3)		78.8	78.8	78.8	78.4

* Standard deviations are ~1 in the final digit.

TABLE 5. REFINED AND CALCULATED SITE-SCATTERING VALUES (EPFU) AT THE CATION SITES

	N*	A(1)	A(2)	A(3)	A(4)
T(1)	4	–	–	63.22	60.55
T(2)	4	–	–	57.87	59.49
M(1)	2	23.97	24.00	23.97	24.07
M(2)	2	23.95	31.73	27.66	33.07
M(3)	1	12.06	12.02	11.96	12.01
Σ*M* (SREF)		59.98	67.75	63.59	69.15
Σ*M* (EMP)		60.02	67.33	63.85	69.09
M(4)	2	36.71	30.33	36.90	39.70
M(4) (EMP)		37.10	30.91	37.59	39.92
A	1	1.07	1.85	1.10	1.41
A(*m*)	2	5.23	5.61	5.54	5.41
A(2)	2	2.79	3.20	3.51	5.41
Σ*A* (SREF)		9.09	10.66	10.15	12.23
Σ*A* (EMP)		8.88	10.56	10.43	12.04
Σ SREF		105.78	108.74	110.64	121.08
Σ EMP		106.00	108.80	111.87	121.05

*N = number of sites in the structural formula
SREF = from single-crystal structure refinement
EMP = from the unit formulae of Table 6.

TABLE 6. CHEMICAL COMPOSITIONS AND UNIT FORMULAE FOR THE AMPHIBOLES OF THIS WORK

	A(1)	A(2)	A(3)	A(4)
SiO_2 wt%	53.95	51.35	48.63	40.31
Al_2O_3	3.74	4.80	3.25	10.98
M_2O_3	–	7.00	7.25	10.61
MgO	24.65	19.39	22.33	18.50
CaO	11.33	6.56	11.15	13.33
Na_2O	3.97	7.21	4.15	2.98
F	4.60	4.50	4.40	4.29
O=F	–1.94	–1.90	–1.75	–1.81
Total	100.30	98.91	99.41	99.19
Chemical formulae				
Si *apfu*	7.419	7.235	7.025	5.984
Al	0.581	0.765	0.503	1.460
M^{3+}	–	–	0.472	0.556
ΣT	8.000	8.000	8.000	8.000
Al	0.025	0.032	0.050	0.461
M^{3+}	–	0.859	0.200	0.454
Mg	4.975	4.073	4.750	4.085
ΣC	5.000	4.964	5.000	5.000
Mg	0.079	–	0.060	0.010
Ca	1.669	0.990	1.726	1.990
Na	0.252	1.010	0.214	–
ΣB	2.000	2.000	2.000	2.000
Ca	–	–	–	0.130
Na	0.807	0.960	0.948	0.858
ΣA	0.807	0.960	0.948	0.988
F	2.001	2.005	2.010	2.014

M = trivalent cations other than Al; A(2) = Sc; A(3) and A(4) = Ga

A-group sites

SREF and EMP results indicate a deficiency of Na at the *A* site, as well as the presence of some ^{A}Ca in crystal *A*(4), as had been observed in synthetic fluoropargasite (Oberti *et al.* 1995a). The refined site-scatterings and the shape of the electron density indicate that Na preferentially occurs at the *A*(*m*) position in crystals A(1), A(2) and A(3) (Fig. 1a), and is disordered between *A*(*m*) and *A*(2) in crystal A(4) (Fig. 1b). Hawthorne *et al.* (1996) showed that the short-range-ordered local configuration $^{M(4)}$Na–$^{O(3)}$F–$^{A(m)}$Na is strongly preferred, and suggested that $^{M(4)}$Ca–$^{O(3)}$F–$^{A(m)}$Na and $^{M(4)}$Ca–$^{O(3)}$F–$^{A(2)}$Na have nearly equal probability. The present results confirm their conclusions.

TABLE 7. PROPOSED FORMULAE (SREF+EMP) FOR THE AMPHIBOLES OF THIS WORK

Sample	Formula												
	A		B			C			T				
A(1)	$Na_{0.82}$		$Na_{0.26}$	$Ca_{1.67}$	$Mg_{0.07}$	$Mg_{4.98}$	$Al_{0.02}$		$Si_{7.42}$	$Al_{0.58}$		O_{22}	F_2
A(2)	$Na_{0.85}$		$Na_{1.02}$	$Ca_{0.98}$		$Mg_{4.14}$	$Sc_{0.86}$		$Si_{7.21}$	$Al_{0.79}$		O_{22}	F_2
A(3)	$Na_{0.94}$		$Na_{0.22}$	$Ca_{1.72}$	$Mg_{0.06}$	$Mg_{4.75}$	$Al_{0.05}$	$Ga_{0.20}$	$Si_{7.03}$	$Al_{0.50}$	$Ga_{0.47}$	O_{22}	F_2
A(4)	$Na_{0.88}$	$Ca_{0.12}$		$Ca_{2.00}$		$Mg_{4.09}$	$Al_{0.46}$	$Ga_{0.45}$	$Si_{5.99}$	$Al_{1.45}$	$Ga_{0.56}$	O_{22}	F_2

T-group sites

Crystals A(1) and A(2) have nominal *T*-group compositions Si_7Al. The <*T*(2)–O> distances indicate no Al at *T*(2) in these crystals, whereas the <*T*(1)–O> distances show that ^{T}Al is completely ordered at *T*(1) in each crystal. Using the relations of Oberti *et al.* (1995b), the <*T*(1)–O> distances of A(1) and A(2) indicate 0.67 and 0.71 ^{T}Al *apfu*, respectively, compared with the ^{T}Al contents from electron-microprobe analysis of 0.58 and 0.77 *apfu*, respectively.

The situation for crystals A(3) and A(4) is considerably more complicated. Although these crystals have nominal *T*-group compositions of Si_7Al and Si_6Al_2, respectively, site-scattering refinement (Table 5) indicates that both these crystals must contain $^{[4]}Ga$ as well as $^{[6]}Ga$. Moreover, the <*T*(1)–O> and <*T*(2)–O> distances indicate that (Al, Ga) occurs at both the *T*(1) and *T*(2) sites (Table 4). The (Si,Al) *versus* Ga occupancies can be derived from the results of site-scattering refinement, and then the Si and Al occupancies can be derived from mean bond-length *versus* ionic-radius considerations using the curves of Oberti *et al.* (1995b) modified for the difference in size between $^{[4]}Al$ and $^{[4]}Ga$. The resulting site-populations for A(3) and A(4) are *T*(1) = 3.12 Si + 0.41 Al + 0.47 Ga, *T*(2) = 3.91 Si + 0.09 Al and *T*(1) = 2.34 Si + 1.30 Al + 0.36 Ga, *T*(2) = 3.65 Si + 0.15 Al + 0.20 Ga *apfu*, respectively. We are not confident about the assignment of the small amounts of Al to *T*(2), as a slight change in the effective radius for $^{[4]}Ga$ could lead to the re-assignment of all $^{T(2)}Al$ to the *T*(1) site in both crystals. However, the partial disorder of Ga over the *T*(1) and *T*(2) sites is in accord with the Rietveld results of Jenkins & Hawthorne (1995) on synthetic amphiboles along the nominal join $Ca_2Mg_5Si_8O_{22}F_2 – NaCa_2(Mg_4Ga)(Si_6Ga_2)O_{22}F_2$.

Oberti *et al.* (1995b) showed that $^{[4]}Al$ is ordered at *T*(1) in amphiboles that crystallized at low temperature, and that disorder of $^{[4]}Al$ over *T*(1) and *T*(2) increases at high temperature (>800°C). In the synthetic fluoro-amphiboles of the present work, $^{[4]}Al$ is completely ordered at *T*(1), despite the high temperature (~1200°C) at which synthesis was initiated. There are two possibilities in this regard: (1) amphibole crystals could re-equilibrate during cooling to 770°C, or (2) the presence of F rather than OH at O(3) affects the ordering of $^{[4]}Al$ over *T*(1) and *T*(2).

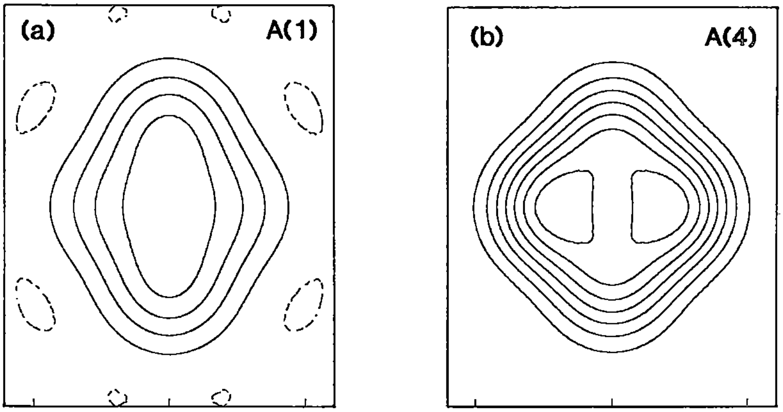

FIG. 1. Difference-Fourier sections (on $\bar{2}01$) through the *A* site, calculated with the *A* cations removed from the structure model; (a) crystal A(1); (b) crystal A(4). The contour interval is 1 *e*/Å ^{3}, and the broken line is the zero contour.

C-group sites

The refined site-scattering values (Table 5) indicate complete ordering of $^{C}M^{3+}$ cations at the *M*(2) site. For crystals A(1) and A(2), the resulting *M*(2) site-populations are in agreement with the unit formulae derived from EMPA data (Table 6). For crystals A(3) and A(4), the refined site-scattering values were used to obtain accurate partitioning of Al and Ga between the *T* and *M* sites.

The <*M*(2)–O> distances correlate well with the mean ionic radius (<r>) of the constituent cations calculated from the site populations (Fig. 2). As $^{[6]}$Al has a smaller radius than $^{[6]}$Ga (0.535 *versus* 0.62 Å), the limited incorporation of Ga at *M*(2) observed in A(3) is not due to dimensional constraints but to its preference for tetrahedral coordination (Jenkins & Hawthorne 1995). The entrance of the large Sc^{3+} cation ($r = 0.745$ Å) increases the distortion of the *M*(2) octahedron, as is the case with synthetic Sc-substituted fluoro-eckermannite (Oberti *et al.* 1999).

<Mg–O,F> DISTANCES IN SYNTHETIC AMPHIBOLES

In all of the crystals examined in the current study, the refined site-scattering values at the *M*(1) and *M*(3) sites are 24.00 (± 0.07) and 12.01 (± 0.05) electrons per formula unit (*epfu*), respectively, indicating that these sites are occupied solely by Mg. This result is in accord with the refined site-scatterings and mean bond-distances at the *M*(2) site, which show that all $^{[6]}M^{3+}$ is ordered at *M*(2). However, the <*M*(1)–O> and <*M*(3)–O> distances reported in Table 4 are significantly different. Table 8 lists the <*M*(1)–O> and <*M*(3)–O> distances available for fluoro-amphiboles with only Mg at *M*(1) and *M*(3), for all of which the actual compositions of the crystal as well as the ordering of octahedrally coordinated cations have been determined. They can be compared also with the ideal <Mg–O,F> distances of 2.051 and 2.044 Å extrapolated for the *M*(1) and *M*(3) sites in fluororichterite ($NaCaNaMg_5Si_8O_{22}F_2$) by Oberti *et al.* (1993).

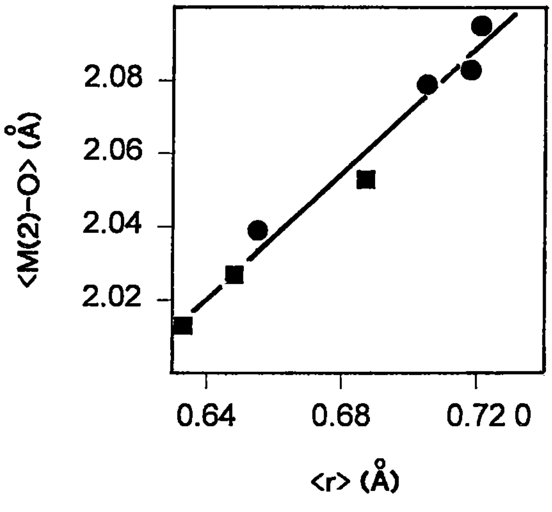

FIG. 2. The dependence of <*M*(2)–O> on the mean cation radius at *M*(2) calculated on the basis of complete $^{[6]}M^{3+}$ ordering at *M*(2); squares are the samples of synthetic fluoropargasite of Oberti *et al.* (1995a) and the synthetic fluoro-edenite of Boschmann *et al.* (1994); the circles represent the data from this paper.

The <*M*(1)–O> distances in the current series of synthetic amphiboles (2.059–2.065 Å; Table 4) are considerably larger than this ideal value, whereas the values reported by Oberti *et al.* (1999) for synthetic sodic and "sodic-cummingtonitic" ($B \approx$ NaMg) fluoro-amphiboles (2.052–2.060 Å) span the difference. The <*M*(3)–O> distances in the current series of amphiboles (2.046–2.052 Å) are in closer agreement, but the values for the samples of Oberti *et al.* (1999) lie in the range 2.045–2.062 Å. Moreover, 2.061 and 2.045 Å have been reported for the <*M*(1)–O> and <*M*(3)–O> distances in nominal synthetic fluoro-edenite (Boschmann *et al.* 1994), and 2.066 and 2.052 Å have been reported for fluoropargasite (Oberti *et al.* 1995a).

As there is no difference in the *M*(1) and *M*(3) cations or the O(3) anion, these differences in <*M*–O> must be inductive, *i.e.*, they are caused by changes at other cation sites in the structure. Until now, we have either ignored such effects in the amphibole structure or have given rather fuzzy "explanations" that have suggested inductive effects. On the other hand, this point cannot be easily addressed in the far more complex natural compositions. It is now apparent from the data discussed above (Table 8) that whatever the cause, the effect on the <Mg–O,F> distances at both *M*(1) and *M*(3) is quite significant: for example, the variation for *M*(1) is 0.013 Å, and this distance corresponds to approximately 0.40 Fe^{2+} *apfu* in terms of variation in <*M*(1)–O> as a function of (Mg,Fe^{2+}) content.

Examination of Table 8 shows some regularity. The calcic and sodic–calcic amphiboles with significant $^{[4]}$Al show longer <*M*(1)–O,F> distances (2.059–2.065 Å) than the sodic amphiboles with no $^{[4]}$Al (2.052–2.053 Å); the "sodic-cummingtonitic" amphiboles show intermediate values (2.056–2.060 Å), whereas the extrapolated value for fluororichterite is 2.051 Å. The aluminous amphiboles are characterized by a dimensionally larger double-chain of tetrahedra because of the presence of $^{[4]}$Al, and hence require a dimensionally larger strip of octahedra. In natural amphiboles, the potential misfit between the two major components of the structure is accommodated by (1) rotation of the double-chain of tetrahedra, which reduces its dimensions, and (2) incorporation of larger cations (particularly Fe^{2+})

in the strip of octahedra. Note that mechanism (1) is affected by the type of *B*-cation(s) occupying the *M*(4) site, whereas the chemical systems of the synthetic amphiboles examined here preclude mechanism (2). In order to accommodate misfit between the double-chain and the strip, the double-chain will rotate, but the bond-valence requirements of the *M*(4) cation and the O(5) and O(6) anions will limit this rotation. Thus, only further expansion or contraction of the polyhedra in the two units can accommodate the residual misfit after rotation of the chain of tetrahedra. As *T*–O bonds are much stronger than *M*–O bonds, most of this "inductive" strain will occur in the strip of octahedra. This is the origin of the variations in <Mg–O,F> in these synthetic fluoro-amphiboles. The large chain of tetrahedra of the calcic samples (with 1.5–2.0 $^{[4]}$Al *apfu*) results in larger <*M*(1)–O> distances as the strip of octahedra is strained to fit with the chain of tetrahedra, whereas the smaller chain of tetrahedra of the sodic samples (with no $^{[4]}$Al) does not require such a strained strip of octahedra. Accordingly, the two crystals containing significant tetrahedrally coordinated Ga ($^{[4]}$Ga = 0.47 Å, $^{[4]}$Al = 0.39 Å) show the longest <*M*(1)–O> distances. The variation in <*M*(3)–O> distances does not show such a correlation, and presumably the *M*(3) octahedron takes a more static role, in line with its lower equipoint rank. This effect of strain is surely much less important in natural amphiboles, as the composition (and hence the size) of the strip of octahedra and the chain of tetrahedra can change almost continuously *via* homovalent substitutions. However, it does suggest why certain compositions (*e.g.*, end-member fluoro-eckermannite) may not be stable: the strain associated with linking the double-chain of tetrahedra to the strip of octahedra exceeds some critical limit.

CONCLUSIONS

The single-crystal structure refinements of synthetic fluoro-amphiboles allows us to state that:

(1) significant deviations from the nominal compositions are nearly always observed and occur at all the groups of sites; therefore, the actual composition of the crystals should always be measured, even if the yield of the desired phase is very high;

(2) in all three Ca–Na amphibole groups, the prevalent substitution for these deviations is $^{B}(\mathrm{Ca,Mg})^{2+} + {}^{C}\mathrm{Mg}^{2+} \rightarrow {}^{B}\mathrm{Na}^{+} + {}^{C}\mathrm{M}^{3+}$; the extent of the substitution does not seem to depend on the size of the $^{C}M^{3+}$ cation;

(3) all $^{C}M^{3+}$ order at the *M*(2) site in fluoro-amphiboles; partitioning over the *M*(2) and the two *T* sites was observed only for Ga in calcic amphiboles;

(4) in terms of atoms per formula unit, most Ga enters the *T* sites in calcic amphiboles. As the two available crystal-chemical mechanisms should behave differently as a function of the P,T conditions of crystallization, this fact has to be taken into account in geochemical studies: only the fraction of Ga occurring in octahedral coordination should be used for the calculation of its partition coefficients, which are to be compared to those of the other lithophile $^{[6]}M^{3+}$ cations;

(5) the *M*–O distances in amphiboles are not a simple function of the constituents of the octahedra, but suffer from inductive effects of the bulk composition. The variations in the <Mg–O,F> distances at the *M*(1) and *M*(3) sites can be interpreted in terms of dimensional misfit between the double-chain of tetrahedra and the strip of octahedra; this effect is exacerbated in these synthetic crystals owing to the non-availability of larger divalent cations such as Fe and Mn (which could be incorporated into the octahedra to reduce the misfit).

TABLE 8. MEAN BOND-LENGTHS AND CHEMICAL FORMULAE OF SYNTHETIC FLUORO-AMPHIBOLES

<M(1)–O> Å	<M(3)–O> Å	Formula (apfu)	Ref.
2.061	2.045	$Na_{0.92}(Ca_{1.92}Na_{0.08})(Mg_{4.64}Al_{0.36})(Si_{6.51}Al_{1.49})O_{22}F_2$	(1)
2.065	2.051	$(Na_{0.85}Ca_{0.20})(Ca_{1.84}Mg_{0.16})(Mg_{4.23}Al_{0.77})(Si_{5.96}Al_{2.04})O_{22}F_2$	(2)
2.059	2.046	$Na_{0.82}(Ca_{1.67}Na_{0.26}Mg_{0.07})(Mg_{4.98}Al_{0.02})(Si_{7.42}Al_{0.58})O_{22}F_2$	(3)
2.059	2.051	$Na_{0.95}(Na_{1.02}Ca_{0.98})(Mg_{4.14}Sc_{0.86})(Si_{7.21}Al_{0.79})O_{22}F_2$	(3)
2.064	2.050	$Na_{0.94}(Ca_{1.72}Na_{0.22}Mg_{0.06})(Mg_{4.75}Ga_{0.20}Al_{0.05})(Si_{7.03}Ga_{0.47}Al_{0.50})O_{22}F_2$	(3)
2.065	2.052	$(Na_{0.88}Ca_{0.12})(Ca_2)(Mg_{4.09}Ga_{0.45}Al_{0.46})(Si_{5.99}Al_{1.45}Ga_{0.56})O_{22}F_2$	(3)
2.060	2.048	$Na_{0.98}(Na_{1.10}Mg_{0.90})(Mg_{4.88}Al_{0.12})(Si_8)O_{22}F_2$	(4)
2.053	2.052	$Na_{0.92}(Na_{1.97}Mg_{0.03})(Mg_{3.95}Sc_{1.05})(Si_8)O_{22}F_2$	(4)
2.059	2.048	$Na_{0.85}(Na_{1.02}Mg_{0.98})(Mg_{4.83}Ti_{0.17})(Si_8)O_{22}F_2$	(4)
2.056	2.045	$Na_{0.90}(Na_{0.92}Mg_{1.08})(Mg_{4.98}V_{0.02})(Si_8)O_{22}F_2$	(4)
2.053	2.062	$Na_{1.00}(Na_{1.97}Mg_{0.03})(Mg_{4.03}Cr_{0.97})(Si_8)O_{22}F_2$	(4)
2.052	2.046	$Na_{1.00}(Na_{1.75}Mg_{0.25})(Mg_{4.25}Cr_{0.75})(Si_8)O_{22}F_2$	(4)
2.057	2.046	$Na_{0.94}(Na_{1.07}Mg_{0.93})(Mg_{4.87}Ga_{0.13})(Si_8)O_{22}F_2$	(4)

References: (1) Boschmann *et al.* (1994); (2) Oberti *et al.* (1995a); (3) this study; (4) Oberti *et al.* (1999)

ACKNOWLEDGEMENTS

FCH and MR were supported by Operating and Major Equipment Grants from the Natural Sciences and Engineering Research Council of Canada. Financial support for FC was provided by a research grant from the Spanish M.E.C. Bernard Evans, David Jenkins, Peter Burns and Bob Martin are gratefully acknowledged for their constructive criticisms during the review process.

REFERENCES

BOSCHMANN, K.F., BURNS, P.C., HAWTHORNE, F.C., RAUDSEPP, M. & TURNOCK, A.C. (1994): A-site disorder in synthetic fluor-edenite, a crystal-structure study. *Can. Mineral.* **32**, 21-30.

HAWTHORNE, F.C., OBERTI, R. & SARDONE, N. (1996): Sodium at the *A* site in clinoamphiboles: the effect of composition on patterns of order. *Can. Mineral.* **34**, 577-593.

JENKINS, D.M. & HAWTHORNE, F.C. (1995): Synthesis and Rietveld refinement of amphibole along the join $Ca_2Mg_5Si_8O_{22}F_2$–$NaCa_2Mg_4Ga_3Si_6O_{22}F_2$. *Can. Mineral.* **33**, 13-24.

OBERTI, R., HAWTHORNE, F.C., CAMARA, F. & RAUDSEPP, M. (1999): Unusual M^{3+} cations in synthetic amphiboles with nominal fluoro-eckermannite composition: deviations from stoichiometry and structural effects of the cummingtonite component. *Am. Mineral.* (in press).

________, ________, UNGARETTI, L. & CANNILLO, E. (1993): The behaviour of Mn in amphiboles: Mn in richterite. *Eur. J. Mineral.* **5**, 43-51.

________, SARDONE, N., HAWTHORNE, F.C, RAUDSEPP, M. & TURNOCK, A.C. (1995a): Synthesis and crystal-structure refinement of synthetic fluor-pargasite. *Can. Mineral.* **33**, 25-31.

________, UNGARETTI, L., CANNILLO, E., HAWTHORNE, F.C. & MEMMI, I. (1995b): Temperature-dependent Al order – disorder in the tetrahedral double chain of *C2/m* amphiboles. *Eur. J. Mineral.* **7**, 1049-1063.

RAUDSEPP, M., TURNOCK, A.C. & HAWTHORNE, F.C. (1991): Amphibole synthesis at low pressure: what grows and what doesn't. *Eur. J. Mineral.* **3**, 983-1004.

________, ________, ________, SHERRIFF, B.L. & HARTMAN, J.S. (1987): Characterization of synthetic pargasitic amphiboles ($NaCa_2Mg_4M^{3+}Si_6Al_2O_{22}(OH,F)_2$; M^{3+} = Al, Cr, Ga, Sc, In) by infrared spectroscopy, Rietveld structure refinement, and ^{27}Al, ^{29}Si, and ^{19}F MAS NMR spectroscopy. *Am. Mineral.* **72**, 580-593.

Received May 15, 1998, revised manuscript accepted September 5, 1998.